Available online at www.sciencedirect.com
SCIENCE DIRECT®
International Journal of Heat and Mass Transfer 47 (2004) 775–785
International Journal of HEAT and MASS TRANSFER
www.elsevier.com/locate/ijhmt

Mass transport regimes in a laminar boundary layer with suction—parallel flow and high Peclet number

João M. Miranda, João B.L.M. Campos *

Centro de Estudos de Fenómenos de Transporte, Departamento de Engenharia Química, Faculdade de Engenharia da Universidade do Porto, Rua Dr. Roberto Frias, 4200-465 Porto, Portugal

Received 20 June 2002; received in revised form 30 June 2003

Abstract

Mass transport in a boundary layer with suction was studied for a parallel flow, laminar regime and high Peclet number. Mass transport mechanisms involved were analyzed and the respective mass transport fluxes were quantified by numerical methods. According to the magnitude of the convective fluxes, mass transport regimes were established. A simple, but accurate equation was deduced to identify the dominant convective flux and the transport regime. This identification only requires measurable variables combined in dimensionless groups. The accuracy of the equation was proved through the numerical solution of the governing flow and mass transport equations. The concentration field inside the mass boundary layer and the concentration polarization level at the permeable surface are intrinsically related with the dominant convective flux. A simple equation was deduced relating the concentration polarization level at the permeable surface and the parameter Ω_{j_z}, which characterizes the transport regime.

Keywords: Mass transport; Fluid mechanics; Laminar flow; Mass boundary-layer with suction

1. Introduction

Mass transfer in a boundary layer over a permeable surface with suction is a relevant topic with a wide range of applications, in particular in membrane separation processes: microfiltration, reverse osmosis and ultrafiltration.

For high Peclet numbers, the mass boundary layer is very thin, and a detailed study of the flow and mass transport mechanisms is complex. Several studies have been done, but there are yet some questions without a definitive answer. How suction modifies the flow inside the mass boundary layer? How the normal velocity component changes inside the mass boundary layer? How the normal convective mass flux is related to the diffusive mass flux promoted by the normal concentration gradient? What is the importance of the transversal convective mass flux to the concentration field inside the boundary layer? Is it possible to know, à priori, the dominant convective mass transport flux inside the boundary layer? These and other questions appear frequently in several works and, in most of them, some simplifications are assumed.

Brian [1] conceptualized the stagnant film model for a permeable plate with suction. This model was built over some flow and mass transport assumptions: the inexistence of transversal velocity component, uniform normal velocity component, and equal normal convective and diffusive mass fluxes. Several authors, Probstein et al. [2], Trettin and Doshi [3] and Zidney [4] discussed the stagnant model and the respective equation, putting in relevance the inaccuracy of the assumptions.

The main drawback to answer to all these questions and to test the validity of the stagnant film equation is the difficulty in measuring the velocity and concentration fields inside the mass boundary layer. Velocity and concentration fields can only be determined by numerical solution of the governing momentum and mass solute balance equations, solved with appropriate boundary conditions. With the numerical predictions, it is possible

* Corresponding author. Tel.: +351-22-508-1692; fax: +351-22-508-1649/1449.
E-mail address: jmc@fe.up.pt (J.B.L.M. Campos).

0017-9310/$ - see front matter © 2003 Elsevier Ltd. All rights reserved.
doi:10.1016/j.ijheatmasstransfer.2003.06.007

Nomenclature

c	normalized solute concentration
c_0	normalized solute concentration in the bulk ($=1$)
c_m	normalized solute concentration at the permeable surface
C	solute concentration (kg/m^3)
C_0	solute concentration in the feed (kg/m^3)
C_m	solute concentration at the permeable surface (kg/m^3)
D	molecular diffusivity (m^2/s)
F_{v_x}	local ratio between the variation of the transversal convective transport and the variation of the normal diffusive transport
F_{v_z}	local ratio between the variation of the normal convective transport and the variation of the normal diffusive transport
H	distance between parallel plates (m)
I_c	concentration polarization index based on the surface concentration
j_z	normalized velocity perturbation in z-direction
k^m	mass transfer coefficient (m/s)
R_m	permeable surface flow resistance (Pa s m^{-1})
v_m	normalized velocity at the permeable surface (m/s)
v_x	normalized transversal velocity component
v_z	normalized normal velocity component
V_0	mean inlet velocity (m/s)
V_m	velocity at the permeable surface (m/s)
V_x	transversal velocity component (m/s)
V_z	normal velocity component (m/s)
x	normalized transversal coordinate
z	normalized normal coordinate
X	tranversal coordinate (m)
Z	normal coordinate (m)

Non-dimensional numbers

Pe	Peclet number $\left(=\frac{HV_0}{D}\right)$
Re	Reynolds number $\left(=\frac{\rho H V_0}{\mu}\right)$
Sh^m	Sherwood number characterizing the mass transfer between the fluid at the permeable surface and the bulk $\left(=\frac{k^m H}{D}\right)$
Sh^m_{ln}	Sherwood number based in the stagnant film theory $\left(=\frac{k^m_{ln} H}{D}\right)$
Sh^i	Sherwood number in an impermeable system $\left(=\frac{k^i H}{D}\right)$
Sh^i_c	Sherwood number in an impermeable system with uniform concentration at the wall $\left(=\frac{k^i_c H}{D}\right)$
Sh^i_f	Sherwood number in an impermeable system with uniform mass production at the wall $\left(=\frac{k^i_f H}{D}\right)$
Π_v	$\frac{\Delta P_m - \pi_0}{R_m V_0}$
Π_{π_0}	$\frac{\pi_0}{\Delta P_m}$
Ω_1	$\frac{Pe\Pi_v}{Sh^m_{ln}}$

Greek symbols

$\delta^{99\%}$	normalized mass boundary layer thickness; distance from the permeable surface to z where the following condition is observed, $(C-C_0)/(C_m-C_0)=0.01$
ΔP_m	static pressure difference across the permeable surface (Pa)
μ	dynamic viscosity of the feed (Pa s)
π_0	osmotic pressure in the liquid over the surface with concentration C_0 (Pa)
ρ	density of the feed solution (kg/m^3)
Ω_{v_z}	mean (along z-direction) amount of mass deviated from the normal diffusive flux by the normal convective flux
Ω_{j_z}	Ω_{v_z}

to compare and to quantify the mass transport mechanisms, to interpret their effects, and to establish mass transfer regimes for any operating conditions.

In this work, an effort is made to deduce a simple equation, with practical utility, which relates the mass transfer regime with the operating conditions. The study is done for a parallel plate cell with a laminar and well-developed flow, and for high Peclet numbers. In the literature, there are several works concerning the numerical prediction of concentration and velocity profiles inside a mass boundary layer with suction: Kleinstreuer and Paller [5], Bhattacharyya et al. [6], Bouchard et al. [7], Bhattacharjee et al. [8], Ganguly and Bhattacharya [9], Bhattacharya and Hwang [10], and De et al. [11]. In spite of this long list, none of these authors analysed the mass transfer mechanisms and the mass transport regimes in the fundamental point of view developed in this work.

In the next section the theory is developed, afterwards the numerical work is briefly described, and at last, the results are presented and discussed.

2. Theoretical analysis

Inside a two-dimensional boundary layer over a permeable surface with suction, the solute transport equation has four terms, each one associated with a mass transport mechanism:

$$v_x \frac{\partial c}{\partial x} + v_z \frac{\partial c}{\partial z} = \frac{1}{Pe}\left[\frac{\partial^2 c}{\partial x^2} + \frac{\partial^2 c}{\partial z^2}\right] \tag{1}$$

where c is the solute concentration normalized by the bulk concentration, v the fluid velocity normalized by the mean velocity of the bulk, x and z the transversal and normal coordinates normalized by the height of the channel, H, and Pe the Peclet number.

The terms on the left side of the equation are associated with mass transport by convection along the tangential, x, and axial, z, directions, while the terms on the right side are associated with mass transport by diffusion along the tangential, x, and axial, z, directions. In a steady mass boundary layer, the concentration gradient in the transversal direction is always much lower than the concentration gradient in the axial direction, this one through the thin mass boundary layer. Therefore, the diffusive transport in the transversal direction is small and can be neglected when compared with the others transport terms. The solute mass transport equation can be re-written without this term:

$$v_x \frac{\partial c}{\partial x} + v_z \frac{\partial c}{\partial z} = \frac{1}{Pe}\frac{\partial^2 c}{\partial z^2} \tag{2}$$

Each term of Eq. (2) can be associated to mass flux differences at the outlet and inlet, the net flux, of an infinitesimal element of volume placed inside the mass boundary layer. For example:

$$\left(v_x \frac{\partial c}{\partial x}\right)\delta x \approx v_x c|_{x+\delta x} - v_x c|_x \tag{3}$$

Fig. 1 shows an infinitesimal volume with the respective mass fluxes entering and leaving the element. In the steady state, the diffusional mass flux at the inlet of the infinitesimal volume, coming from the permeable surface, is always higher than the diffusional mass flux leaving the infinitesimal volume, going into the direction of the bulk. This decrease must be balance by an increase of the transversal convective transport and/or of the normal convective transport, i.e.:

the net diffusing flux in the volume of control

= the net normal convective flux

+ the net transversal convective flux

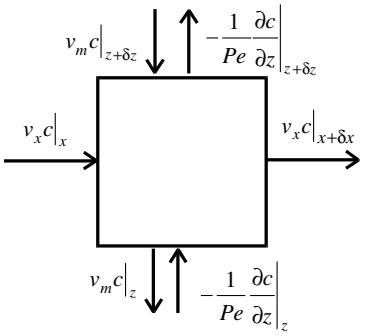

Fig. 1. Infinitesimal control volume inside the mass boundary layer.

An appropriate picture is the departure by convection of some of the mass traveling by diffusion from the permeable surface to the bulk. This mass is incorporated into the normal convective flux, returning to the surface, and/or into the transversal convective flux, spreading along the boundary layer. The concentration profiles in the boundary layer depend on which mechanism is the most "powerful" to deviate the mass traveling by diffusion. If it is the convective transport in the normal direction, the solute concentration over the permeable surface is high and the mass gradients, in axial and transversal directions, are high. If it is the convective transport in the transversal direction, the solute concentration over the surface is low and the mass gradients, in both directions, are low.

The "strength" of the convective mechanisms is the source of the mass transfer regimes inside the mass boundary. Therefore, it is important to have a parameter, with physical meaning, to quantify the "strength" of the convective mechanisms. With this purpose, a parameter was defined which weights the variation of the transversal convective transport, first term of Eq. (2), with respect to the variation of the normal diffusive transport, third term of Eq. (2):

$$F_{v_x} = \frac{\dfrac{\partial (v_x c)}{\partial x}}{\dfrac{1}{Pe}\dfrac{\partial^2 c}{\partial z^2}} \tag{4}$$

Another parameter could be defined, weighting the variation of the normal convective transport, second term of Eq. (2), in respect to the variation of the normal diffusive transport, third term of Eq. (2):

$$F_{v_z} = \frac{\dfrac{\partial (v_z c)}{\partial z}}{\dfrac{1}{Pe}\dfrac{\partial^2 c}{\partial z^2}} \tag{5}$$

According to Eq. (2), the sum of these two parameters must be equal to one:

$$F_{v_x} + F_{v_z} = 1 \tag{6}$$

The mean relative amount of mass deviated inside the boundary layer by normal convection is given integrating each term of the ratio F_{v_z} along the normal direction:

$$\Omega_{v_Z} = \frac{\int_0^{\delta} \frac{\partial(v_z c)}{\partial z}\,\mathrm{d}z}{\int_0^{\delta} \frac{1}{Pe}\frac{\partial^2 c}{\partial z^2}\,\mathrm{d}z} \tag{7}$$

The integration of the normal convective term is possible if, inside the mass boundary layer, the normal fluid velocity, v_z, is uniform along z. In a developed laminar flow between two parallel plates, the magnitude of the normal velocity component is equal to the normal perturbation induced in the flow by the suction, since the normal velocity component in the analogous impermeable device is zero. This velocity perturbation is going to be designated by j_z (normalized by the mean velocity in the bulk). If this velocity/perturbation is uniform along the normal direction, it must be equal to the normalized permeate velocity, v_m (the normal velocity at $z = 0$).

$$\Omega_{j_z} = \frac{\int_0^{\delta} \frac{\partial(j_z c)}{\partial z}\,\mathrm{d}z}{\int_0^{\delta} \frac{1}{Pe}\frac{\partial^2 c}{\partial z^2}\,\mathrm{d}z} = \frac{\int_{j_z c_\mathrm{m}}^{j_z c_0} \partial(j_z c)}{\frac{1}{Pe}\int_0^{\delta} \partial\frac{\partial c}{\partial z}\,\mathrm{d}z} \tag{8}$$

or

$$\Omega_{j_z} = \frac{\int_0^{\delta} \frac{\partial(j_z c)}{\partial z}\,\mathrm{d}z}{\int_0^{\delta} \frac{1}{Pe}\frac{\partial^2 c}{\partial z^2}\,\mathrm{d}z} = \frac{\int_{j_z c_\mathrm{m}}^{j_z c_0} \partial(j_z c)}{\frac{1}{Pe}\int_{\frac{\partial c}{\partial z}\big|_{z=0}}^{0} \partial\frac{\partial c}{\partial z}} = \frac{j_z(c_\mathrm{m} - c_0)}{\frac{1}{Pe}\frac{\partial c}{\partial z}\Big|_{z=0}} \tag{9}$$

where δ is the normalized mass boundary layer thickness, c_0 the normalized concentration in the bulk ($c_0 = 1$), and c_m the normalized concentration at the permeable surface.

By definition, the Sherwood number characterizing the mass transfer between the fluid over the permeable surface and the bulk, Sh^m, is given by:

$$Sh^\mathrm{m} = -\frac{\frac{\partial c}{\partial z}\Big|_{z=0}}{(c_s - c_0)} \tag{10}$$

and combining Eqs. (9) and (10):

$$\Omega_{j_z}(x) = -\frac{j_z(x) Pe}{Sh^\mathrm{m}(x)} \tag{11}$$

Assuming total solute retention at the permeable surface, Sh^m can be related with j_z through a simple mass balance at the permeable surface:

$$-V_\mathrm{m} C_\mathrm{m} = k^\mathrm{m}(C_\mathrm{m} - C_0) \tag{12}$$

where the permeate velocity, V_m, is negative according to the coordinate system.

The previous equation can be rewritten taking normalized variables:

$$j_z(x) = -\frac{Sh^\mathrm{m}(x)}{Pe}[1 - 1/c_\mathrm{m}(x)] \tag{13}$$

Combining Eqs. (11) and (13), it follows:

$$\Omega_{j_z}(x) = 1 - 1/c_\mathrm{m}(x) \tag{14}$$

The parameter defining the regime, $\Omega_{j_z}(x)$, is related, in the above equation, with the solute concentration at the permeable surface. The solute concentration is difficult to be known or calculated, and so the next step is to relate the parameter $\Omega_{j_z}(x)$ with other parameters of easier quantification.

Lonsdale et al. [12] expressed the normalized permeate velocity by the ratio between the pressure driving force and the resistance to the flow imposed by the permeable surface:

$$v_\mathrm{m}(x) = j_z(x) = -\frac{\Delta P_\mathrm{m}(x) - \Delta\pi(x)}{V_0 R_\mathrm{m}} \tag{15}$$

According to the dimensional analysis performed by Miranda and Campos [13], the normalized permeate velocity can be expressed by the following equation:

$$v_\mathrm{m}(x) = j_z(x) = -\frac{\Pi_v}{1 - \Pi_{\pi_0}}[1 - c_\mathrm{m}(x)\Pi_{\pi_0}] \tag{16}$$

where Π_v represents the ratio between the permeate velocity through a non-polarized surface and the mean velocity characteristic of the flow, $\Pi_v = \frac{\Delta P_\mathrm{m} - \pi_0}{R_\mathrm{m} V_0}$, and Π_{π_0} represents the ratio between the osmotic pressure over a non-polarized surface and the static pressure difference across the surface, $\Pi_{\pi_0} = \frac{\pi_0}{\Delta P_\mathrm{m}}$.

Combining Eqs. (13) and (16), it is possible to relate c_m with measurable parameters. Substituting the result of this combination in Eq. (14), it yields an implicit equation in Ω_{j_z}:

$$\Omega_{j_z}(x) = \frac{\Pi_v Pe}{Sh^\mathrm{m}(x)(1 - \Pi_{\pi_0})}\left(1 - \frac{\Pi_{\pi_0}}{1 - \Omega_{j_z}(x)}\right) \tag{17}$$

Almost all the dimensionless groups in Eq. (17) can be quantified through the operating conditions, except Sh^m. In the literature, Sherwood number based on the stagnant film theory, $Sh^\mathrm{m}_\mathrm{ln}$, is frequently employed in alternative to Sh^m. According to the stagnant film theory, $Sh^\mathrm{m}_\mathrm{ln}$ is given by:

$$Sh^\mathrm{m}_\mathrm{ln}(x) = -\frac{Pe\, j_z(x)}{\ln c_\mathrm{m}(x)} \tag{18}$$

From Eqs. (11), (14) and (18), a relationship between Sherwood numbers is obtained:

$$\frac{Sh^\mathrm{m}_\mathrm{ln}(x)}{Sh^\mathrm{m}(x)} = \frac{\Omega_{j_z}(x)}{\ln\frac{1}{1 - \Omega_{j_z}(x)}} \tag{19}$$

The substitution of Sh^m by $Sh^\mathrm{m}_\mathrm{ln}$ in Eq. (17) gives:

$$\ln\frac{1}{1 - \Omega_{j_z}(x)} = \frac{\Omega_1(x)}{1 - \Pi_{\pi_0}}\left(1 - \frac{\Pi_{\pi_0}}{1 - \Omega_{j_z}(x)}\right) \tag{20}$$

where:

$$\Omega_1(x) = \frac{\Pi_v Pe}{Sh^\mathrm{m}_\mathrm{ln}(x)} \tag{21}$$

Eq. (20) is the desired equation; an implicit equation relating the fraction of the normal diffusive flux deviated by the normal convective flux with measurable dimensionless parameters.

According to Miranda and Campos [14], the values of $Sh_{\ln}^{m}$ are well approximated by Sherwood data obtained in impermeable systems with similar geometry, $Sh^{i}(x)$:

$$\Omega_1(x) = \frac{\Pi_v Pe}{Sh_{\ln}^{m}(x)} \approx \frac{\Pi_v Pe}{Sh^{i}(x)} \tag{22}$$

The accuracy of this assumption will be discussed later.

3. Numerical procedure

An improved finite-difference scheme was used to solve the momentum and solute mass transport equations. This improved numerical scheme is described in detailed in Miranda and Campos [15]. Only the basic principles are going to be briefly described.

For high Peclet number systems, the mass boundary layer is very thin and to achieve accurate numerical solutions, a very dense grid near the permeable surface must be used. Inside the boundary layer, the solute concentration changes intensely, in particular for high permeate fluxes; the first and second derivatives in order to the normal direction are high. The shape of the concentration profiles is close to exponential and so a variable transformation, $\theta = \ln c$, was used to attenuate those derivatives. Applying this transformation, the shape of the θ profiles becomes almost linear and accurate solutions are obtained with large grid spacing. The orthogonal grid used was denser at the beginning and at the end of the numerical domain, and in the layer over the surface, where concentration and velocity gradients have their highest values.

The flow and θ equations were discretized by a finite difference technique. The θ equation was transformed before discretization. After discretization, an iterative numerical method was used to solve the discretized equations. The convergence of the iterative process was studied by two complementary ways: analyzing the evolution of the θ values in the layer adjacent to the surface, and analyzing the sum of the normalized total residues of the discretized θ equation and respective boundary conditions. The accuracy of the numerical method was tested obtaining solutions on successively refined grids.

4. Validation of the theoretical analysis

4.1. Normal velocity component in the mass boundary layer

The theory developed is supported on the assumption that the normal velocity component, j_z, is uniform inside the mass boundary layer and equal to the permeate velocity. To show the accuracy of this assumption, the velocity field was simulated for different values of Reynolds and Π_v numbers with $\Pi_{\pi_0} = 0$. Taking these predictions, lines of equal ratio j_z/v_m were plotted along x (Fig. 2(a)–(c)).

A line representing the upper limit of the mass boundary layer was also plotted along x, the dark line in Fig. 2(a)–(c). The mass boundary layer thickness, $\delta^{99\%}$, depends on Peclet, Π_v and Π_{π_0} numbers. The line represented is for the highest value of $\delta^{99\%}$ in the range of operating conditions studied, i.e., for the lowest Peclet number, $Pe = 10^5$, the highest Π_v number, $\Pi_v = 2 \times 10^{-4}$, and $\Pi_{\pi_0} = 0$.

Fig. 2(a) shows data for a low Reynolds number, $Re = 100$, and a high Π_v number, $\Pi_v = 2 \times 10^{-4}$. Along the permeable surface, the value of the ratio j_z/v_m is

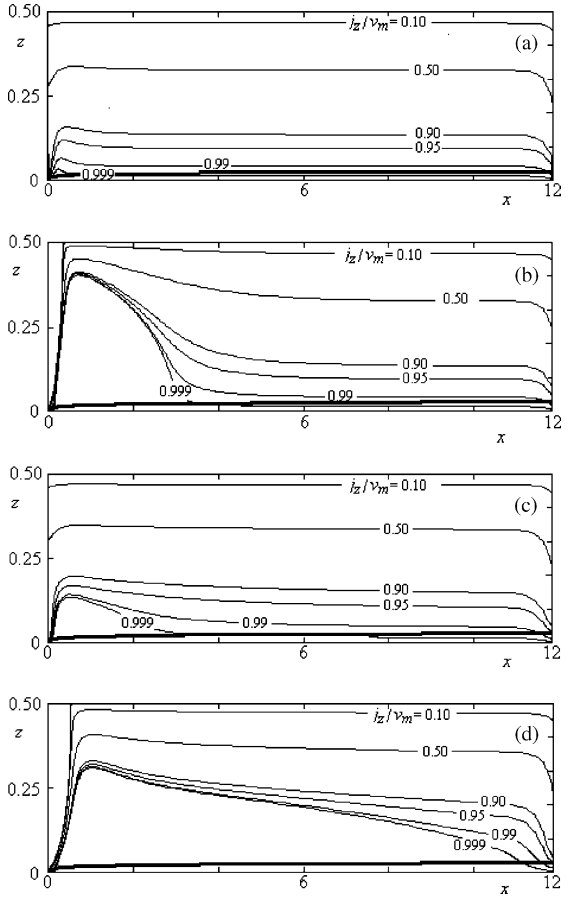

Fig. 2. Flow maps representing j_z/v_m in the vicinity of a permeable surface: (a) $Re = 100$, $\Pi_v = 2 \times 10^{-4}$ and $\Pi_{\pi_0} = 0$; (b) $Re = 100$, $\Pi_v = 10^{-6}$ and $\Pi_{\pi_0} = 0$; (c) $Re = 2000$, $\Pi_v = 2 \times 10^{-4}$ and $\Pi_{\pi_0} = 0$; (d) $Re = 2000$, $\Pi_v = 10^{-6}$ and $\Pi_{\pi_0} = 0$. The dark line represents the upper limit of the mass boundary layer, $Pe = 10^5$, $\Pi_v = 2 \times 10^{-4}$ and $\Pi_{\pi_0} = 0$.

equal to unity and decreases for increasing values of z. For values of z lower than 0.05, the ratio j_z/v_m is lower than 0.99, i.e., from the plate until a distance equal to 5% the height of the channel, the normal velocity is almost uniform and equal to v_m.

Fig. 2(b) shows data for a low Reynolds number, $Re = 100$, and a low Π_v number, $\Pi_v = 10^{-6}$. The flow map is identical to the previous one except in the initial zone of the surface. This different behavior is consequence of the flow region perturbed by the suction. While for high Π_v numbers, the flow is perturbed in a region preceding the permeable surface, for low Π_v numbers, the flow is perturbed very close to the beginning of the permeable surface. From this zone on, the flow map is identical to the previous one.

Fig. 2(c) shows data for a high Reynolds number, $Re = 2000$, and a high Π_v number, $\Pi_v = 2 \times 10^{-4}$. Comparing Fig. 2(a) and (c), it can be observed a small change of the flow field at the beginning of the permeable surface, consequence of the magnitude of the Reynolds number. The distance from the surface to the line representing $j_z/v_m = 0.99$ increases with increasing Reynolds number.

Fig. 2(d) shows data for a high Reynolds number, $Re = 2000$, and a low Π_v number, $\Pi_v = 10^{-6}$. The distance from the surface to the line representing $j_z/v_m = 0.99$ increases with decreasing Π_v number.

In all the previous figures, the thickness (an upper estimative) of the mass boundary layer is always lower than the distance to the surface of the line representing $j_z/v_m = 0.99$. Therefore, the normal velocity component can be taken uniform inside the boundary layer, along z, with an approximation less than 1%.

4.2. Sherwood number in permeable and impermeable systems

The approximation expressed in Eq. (22) is accurate if the Sherwood number based on the stagnant film equation, Sh^m_{ln}, is well estimated by the Sherwood number obtained in an impermeable system with identical geometry, Sh^i. According to Miranda and Campos [14], for low values of Π_{π_0}, Sh^m_{ln} is well estimated by Sh^i data from an impermeable system with uniform mass production at the wall, Sh^i_f, while for high values of Π_{π_0}, ($\Pi_{\pi_0} \to 1$), Sh^m_{ln} is better estimated by Sh^i data from an impermeable system with uniform concentration at the wall, Sh^i_c. To study the accuracy of this approximation, the Sherwood number based on the stagnant film equation, Sh^m_{ln}, was calculated through Eq. (18). The concentration and permeate velocity were obtained from the numerical solution of the flow and mass governing equations. The Sherwood number for an impermeable surface, Sh^i_f or Sh^i_c, was also numerically predicted.

Fig. 3(a) shows Ω_{j_z} data predicted by Eq. (20) employing values of Sh^m_{ln} and values of Sh^i_f, for different values of Π_v, with $Pe = 10^6$ and $\Pi_{\pi_0} = 0$. The deviation between comparable curves increases with increasing Π_v values. The maximum relative deviation observed is around 5% for $\Pi_v = 2 \times 10^{-4}$.

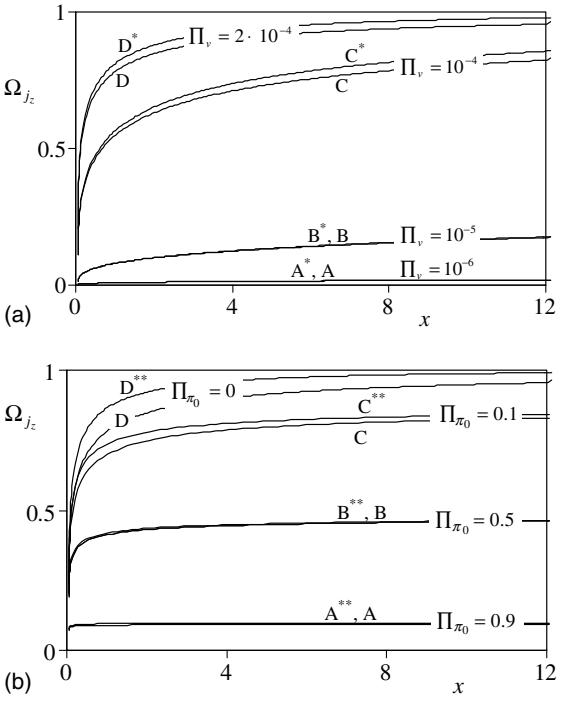

Fig. 3. (a) Ω_{j_z} data predicted by Eq. (20) employing values of Sh^m_{ln} (A, B, C, and D) and of Sh^i_f (A*, B*, C*, and D*) for different values of Π_v, with $Pe = 10^6$ and $\Pi_{\pi_0} = 0$. (b) Ω_{j_z} data predicted by Eq. (20) employing values of Sh^m_{ln} (A, B, C, and D) and of Sh^i_c (A**, B**, C** and D**), for different values of Π_{π_0}, with $Pe = 10^6$ and $\Pi_v = 2 \times 10^{-4}$.

Fig. 3(b) shows Ω_{j_z} data predicted by Eq. (20) employing values of Sh^m_{ln} and values of Sh^i_c, for different values of Π_{π_0}, with $Pe = 10^6$ and $\Pi_v = 2 \times 10^{-4}$. The deviation between comparable curves decreases with increasing Π_{π_0} values. The maximum relative deviation observed is around 10% for $\Pi_{\pi_0} = 0$.

Fig. 3(a) and (b) are illustrative of the accuracy of Eqs. (20) and (22) to quantify the fraction of the normal diffusive flux deviated by the normal convective flux, Ω_{j_z}, inside a mass boundary layer with suction.

5. Mass transport regimes

Mass transport regimes inside the mass boundary layer were studied by numerical simulation. Whatever is the mass transport regime, the following conditions are always observed:

- at the permeable surface, the transversal velocity is zero due to the non-slip condition and the normal

convective flux must be equal to the normal diffusive flux;
- the value of the normal convective flux (normalized) at the upper limit of the mass boundary layer is j_z (the normalized concentration is 1);
- as a result of the mass boundary layer definition, the concentration gradient and the diffusive mass flux are zero at the upper limit of the boundary layer.

According to these conditions, some broad considerations about concentration gradients and mass fluxes inside the mass boundary layer can be stated:

- the diffusive flux must decrease continually from the surface, where it has a maximum value, until the upper limit of the boundary layer where its value is zero;
- the normal convective flux must increase continually from the upper limit of the boundary layer, where it has a minimum value, until the permeable surface where it has a maximum value.

5.1. Uniform permeable velocity ($\Pi_{\pi_0} = 0$)

5.1.1. Transversal regime ($\Omega_{j_z} \leqslant 0.25$)

Fig. 4(a) shows simulation data for $x = 2.0$, $Pe = 10^6$, $\Pi_v = 10^{-5}$ and $\Pi_{\pi_0} = 0$. In the ordinate axis are represented approximated values of each derivative of the mass transport equation (2), namely:

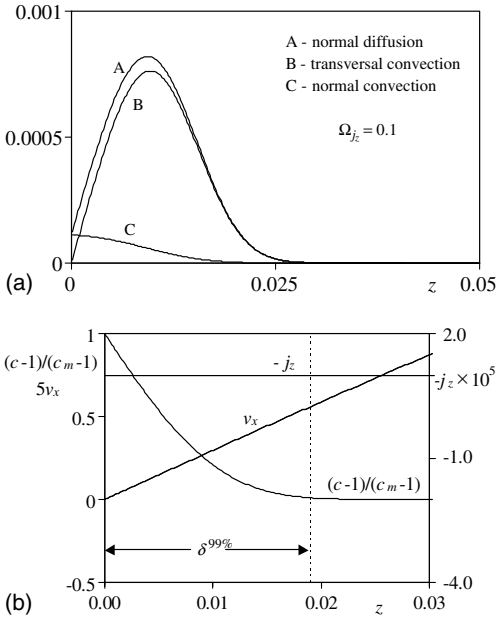

Fig. 4. (a) Approximated values of each derivative of the mass transport equation versus z in the transversal regime, $\Omega_{j_z} = 0.1$; $x = 2.0$, $Pe = 10^6$, $\Pi_v = 10^{-5}$ and $\Pi_{\pi_0} = 0$. (b) Concentration profile and velocity components in the transversal regime, $\Omega_{j_z} = 0.1$; $x = 2.0$, $Pe = 10^6$, $\Pi_v = 10^{-5}$ and $\Pi_{\pi_0} = 0$.

$$\frac{1}{Pe}\left(\frac{\partial^2 c}{\partial z^2}\right) \quad \text{(Curve A—second order approximation)}$$

$$\left(v_x \frac{\partial c}{\partial x}\right) \quad \text{(Curve B—first order approximation)}$$

$$\left(v_z \frac{\partial c}{\partial z}\right) \quad \text{(Curve C—first order approximation)}$$

For these operating conditions, the value of Ω_{j_z}, Eqs. (20) and (21), is 0.1. According to the definition of this parameter, the area below curve C is 10% of the area below curve A and the area below curve B is 90% of the area below curve A.

Analyzing Fig. 4(a), it can be observed that:

- the variation of the convective tangential flux (curve B) is higher than the variation of the convective normal flux (curve C);
- in a substantial part of the boundary layer, the variation of the convective tangential flux (curve B) is identical to the variation of the normal diffusive flux (curve A).

Some conclusions can be taken combining the previous observations with the considerations about the concentration gradients and mass fluxes stated at the beginning of this section:

- 90% of the mass transported by diffusion from the permeable surface is incorporated into the transversal convective flux and is transported along the flow;
- 10% of the mass transported by diffusion from the permeable surface is incorporated into the normal convective flux and return to the surface;
- the normal convective flux increases just near the permeable surface, i.e., the small amount of mass deviated from the diffusional flux is incorporated just over the permeable surface;
- the highest increase of the transversal convective flux is at the middle of the mass boundary layer.

The consequences of this high amount of mass transported in the transversal direction and small amount of mass returning to the permeable surface are: low solute concentration at the surface and low concentration gradients (along z and x) inside the mass boundary layer.

Fig. 4(b) shows, for $x = 2.0$, the velocity components and the concentration profile inside the mass boundary layer. The magnitude of the transversal velocity component is much higher than the magnitude of the normal component. The concentration at the permeable surface is 10% higher than the concentration at the bulk (this value can not be observed in the figure by a question of data representation). The concentration variation along z is slow and extends from the surface until almost the upper limit of the mass boundary layer.

The limit, $\Omega_{j_z} \leqslant 0.25$, chosen for this regime, only means that the mass deviated by the transversal convective flux is at least 3 times greater than the mass deviated by the normal convective flux.

5.1.2. Normal regime ($\Omega_{j_z} \geqslant 0.75$)

Fig. 5(a) shows the simulation data for $x = 3.4$, $Pe = 10^6$, $\Pi_v = 2 \times 10^{-4}$ and $\Pi_{\pi_0} = 0$. Curves A, B and C have the same meaning as those in Fig. 4(a).

For these operating conditions, the value of Ω_{j_z}, Eqs. (20) and (21), is 0.9. According to the definition of this parameter, the area below curve C is 90% of the area below curve A and the area below curve B is 10% of the area below curve A.

Analyzing Fig. 5(a), it can be observed that:

- the variations of the fluxes along the boundary layer are much higher in the normal regime than in the transversal regime;
- the variation of the transversal flux increases slightly at a short distance from the surface and maintains a low value along z;
- the variations of the normal convective flux and of the normal diffusive flux decrease in a similar way, from the surface to the upper limit of the boundary layer.

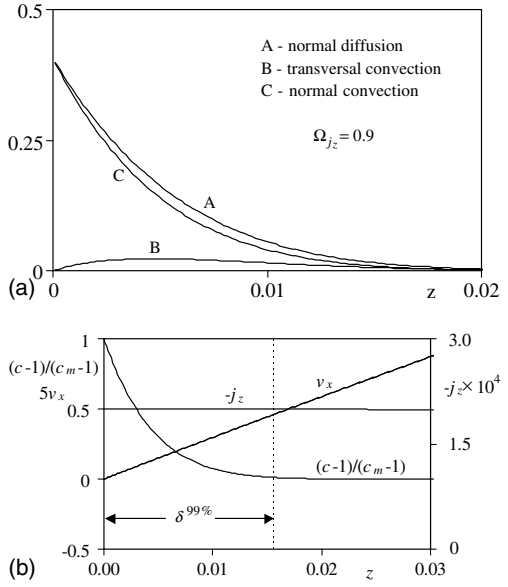

Fig. 5. (a) Approximated values of each derivative of the mass transport equation versus z in the normal regime, $\Omega_{j_z} = 0.9$; $x = 3.4$, $Pe = 10^6$, $\Pi_v = 2 \times 10^{-4}$ and $\Pi_{\pi_0} = 0$. (b) Concentration profile and velocity components in the normal regime, $\Omega_{j_z} = 0.9$; $x = 3.4$, $Pe = 10^6$, $\Pi_v = 2 \times 10^{-4}$ and $\Pi_{\pi_0} = 0$.

Some conclusions can be taken combining the previous observations with the considerations about the concentration gradients and the mass fluxes stated at the beginning of this section:

- 90% of the mass transported by diffusion from the permeable surface is incorporated into the normal convective flux and returns to the permeable surface;
- 10% of the mass transported by diffusion from the permeable surface is incorporated into the transversal convective flux and is transported along the flow;
- the transversal convective flux increases more or less uniformly across the mass boundary layer;
- the highest increase of the normal convective flux is at the permeable surface.

The consequences of this difficult transversal transport and high amount of mass incorporated into the normal convective flux are: high solute concentration at the permeable surface and high concentration gradients (along z and x) inside the boundary layer.

Fig. 5(b) shows, for $x = 3.4$, the velocity components and the concentration profile along z inside the mass boundary layer. The normal velocity component is one order of magnitude higher than in the transversal regime. The concentration at the permeable surface is 920% higher than the concentration at the bulk (this value cannot be observed in the figure by a question of data representation). The concentration variation along z is high until the middle of the mass boundary layer ($z \approx 0.008$) and insignificant from the middle until the upper limit.

The limit, $\Omega_{j_z} \geqslant 0.75$, chosen for this regime, only means that the mass deviated by the normal convective flux is at least three times greater than the mass deviated by the transversal convective flux.

5.1.3. Intermediate regime ($0.25 \leqslant \Omega_{j_z} \leqslant 0.75$)

Fig. 6(a) shows the simulation data for $x = 0.7$, $Pe = 10^6$, $\Pi_v = 10^{-4}$ and $\Pi_{\pi_0} = 0$. Curves A, B and C have the same meaning as those represented in Figs. 4(a) and 5(a).

For these operating conditions, the value of Ω_{j_z}, Eqs. (20) and (21), is 0.5. According to the definition of this parameter, the area below curve C is 50% of the area below curve A and the area below curve B is 50% of the area below curve A.

Analyzing the figure, it can be observed that:

- the variations of the fluxes across the boundary layer are much lower in the intermediate regime than in the normal regime, but are higher than in the transversal regime;
- the variation of the transversal flux increases until the middle of the mass boundary layer where it reaches a maximum value and after decreases until the upper limit;

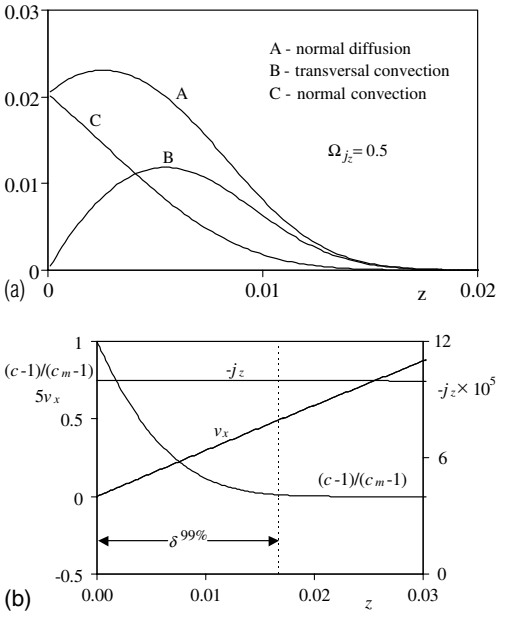

Fig. 6. (a) Approximated values of each derivative of the mass transport equation versus z in the intermediate regime, $\Omega_{j_z} = 0.5$; $x = 0.7$, $Pe = 10^6$, $\Pi_v = 10^{-4}$ and $\Pi_{\pi_0} = 0$. (b) Concentration profile and velocity components in the intermediate regime, $\Omega_{j_z} = 0.5$; $x = 0.7$, $Pe = 10^6$, $\Pi_v = 10^{-4}$ and $\Pi_{\pi_0} = 0$.

- the variation of the normal convective flux decreases from the permeable surface until the upper limit of the mass boundary layer.

Some conclusions can be taken combining the previous observations with the considerations about the concentration gradients and the mass fluxes stated at the beginning of this section.

- 50% of the mass transported by diffusion from the permeable surface is incorporated into the normal convective flux and 50% is incorporated into the transversal convective flux;
- the highest increase of the transversal convective flux is at the middle of the mass boundary layer;
- the highest increase of the normal convective flux is at the permeable surface.

Fig. 6(b) shows, for $x = 0.7$, the velocity components and the concentration profile inside the mass boundary layer. An intermediate behavior between tangential and normal regimes can be observed.

5.2. Variable permeate velocity ($\Pi_{\pi_0} \neq 0$)

The previous analysis was for uniform permeate velocity along x, condition observed when $\Pi_{\pi_0} = 0$, i.e., for a non-polarized permeable surface. Fig. 7 shows the

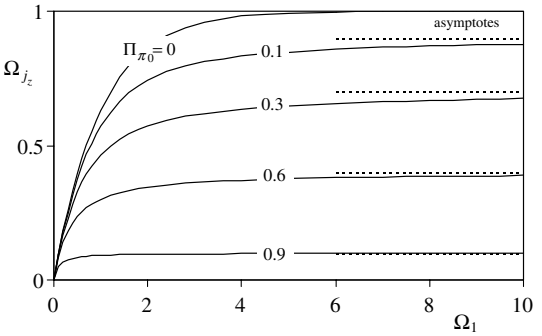

Fig. 7. Ω_{j_z} data versus Ω_1, Eq. (20) with Ω_1 defined by Eq. (21), for different values of Π_{π_0}.

parameter Ω_{j_z} plotted versus Ω_1, Eqs. (20) and (21), for different values of Π_{π_0}. Several interesting conclusions can be taken from this figure:

- for a given value of Π_{π_0}, the mass transported by normal convection increases with increasing values of Ω_1, i.e., with increasing vales of Pe and Π_v, and decreasing values of $Sh_{\ln}^{m}$. However, this increase is significant only for values of $\Omega_1 < 2.0$. From there on Ω_{j_z} tends asymptotically for a constant value;
- the normal regime ($\Omega_{j_z} \geqslant 0.75$) is observed in a straight range of operating conditions, $0 \leqslant \Pi_{\pi_0} \leqslant 0.2$. For $\Pi_{\pi_0} = 0$, the normal regime is observed if $\Omega_1 \geqslant 1.5$ and for $\Pi_{\pi_0} = 0.2$, the normal regime is observed if $\Omega_1 \geqslant 4.0$;
- the normal convective transport decreases strongly with increasing values of Π_{π_0}. For $\Pi_{\pi_0} \geqslant 0.4$, whatever is the value of Ω_1, the transversal convective transport is always higher than the normal convective transport ($\Omega_{j_z} \leqslant 0.5$);
- the transversal regime ($\Omega_{j_z} \leqslant 0.25$) is observed in a large range of operating conditions. For values of Π_{π_0} between 0.7 and 1.0, the regime is transversal whatever the value of Ω_1.

5.2.1. Regimes and concentration polarization

Miranda and Campos [13] defined adequate polarization indexes based on limit concentration and velocity conditions. The concentration index was defined by the following ratio:

$$I_c = \frac{c_m - 1}{1/\Pi_{\pi_0} - 1} \tag{23}$$

where the numerator expresses the difference between the actual surface concentration and the minimum surface concentration, and the denominator all the surface concentration range.

The concentration polarization is an important phenomenon in membrane separation processes and so it is important to know how mass transport regimes and

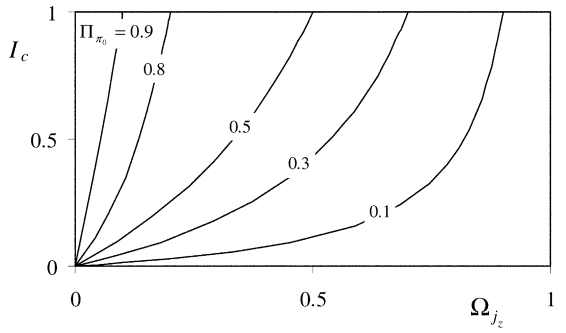

Fig. 8. Polarization concentration index I_c versus Ω_{j_z}, Eq. (24), for several values of Π_{π_0}.

polarization concentration level are related. Combining Eqs. (14) and (23) a relationship between I_c and Ω_{j_z} is found:

$$I_c = \frac{\Omega_{j_z}}{(1-\Omega_{j_z})\left(\frac{1}{\Pi_{\pi_0}}-1\right)} \tag{24}$$

Fig. 8 shows the concentration index I_c versus Ω_{j_z} for several values of Π_{π_0} $(0 < \Pi_{\pi_0} < 1)$. For low values of Π_{π_0}, for example $\Pi_{\pi_0} = 0.1$, the polarization index begins to be low in the transversal and intermediate regimes (low values of Ω_1) and increases strongly in the normal regime (high values of Ω_1). For increasing values of Π_{π_0}, the regime tends to be transversal in all the range of Ω_1 (condition observed for $\Pi_{\pi_0} \geqslant 0.7$), the concentration gradients along x and y directions decrease and the polarization index increases, strongly, with Ω_1.

6. Conclusions

After this work, the convective mass transport fluxes inside a laminar mass boundary layer over a permeable surface with suction can be easily compared. A simple implicit equation, Eq. (20), was deduced relating the fraction of the normal diffusive flux deviated by the normal convective flux, Ω_{j_z}, with measurable dimensionless variables: Pe, Π_{π_0}, Π_v and Sh^i. According to the dominant convective flux, different mass transport regimes were established: normal regime, $\Omega_{j_z} \geqslant 0.75$, transversal regime $\Omega_{j_z} \leqslant 0.25$, and intermediate regime $0.25 \leqslant \Omega_{j_z} \leqslant 0.75$.

The questions stated in the introduction of this work can be definitively answered:

- the suction perturbs the flow in a narrow region very close to the permeable surface and the extension of this region depends on Reynolds and Π_v numbers;
- the normal velocity component is, whatever the operating conditions, uniform inside the mass boundary layer;
- the normal convective flux and the normal diffusive flux are not equal inside the mass boundary layer, as some authors refer;
- the amount of the normal diffusive flux deviated by each convective flux can be calculated by Eqs. (20) and (22), and to do so, only measurable operating variables are needed;
- the transversal convective flux tends to flat and smooth the concentration profiles in both directions, x and z, inside the mass boundary layer;
- the polarization concentration level in a separation membrane can be related with the mass transport regime inside the mass boundary layer, Eq. (24).

Acknowledgements

The authors acknowledge the financial support given by JNICT, PBIC/C/CEN/1337/92 and by F.C.T., PRAXIS XXI/BD/3280/94 and PRAXIS/C/EQU/12141/98.

References

[1] P. Brian, Mass transport in reverse osmosis, in: U. Merten (Ed.), Desalination by Reverse Osmosis, MIT Press, Cambridge, MA, 1964.
[2] R.F. Probstein, J.S. Shen, W.F. Leung, Ultrafiltration of macromolecular solutions at high polarization in laminar channel flow, Desalination 24 (1978) 1–16.
[3] D.R. Trettin, M.R. Doshi, Ultrafiltration in an unstirred batch cell, Industrial and Engineering Chemistry Fundamentals 19 (1980) 189–205.
[4] A.L. Zydney, Stagnant film model for concentration polarization in membrane systems, Journal of Membrane Science 130 (1997) 275–281.
[5] C. Kleinstreuer, M.S. Paller, Laminar dilute suspensions flows in plate and frame ultrafiltration units, AIChE Journal 29 (1983) 529–541.
[6] D. Bhattacharyya, S.L. Backg, R.I. Kermode, S.L. Roco, Prediction of concentration polarization and flux behaviour in reverse osmosis by numerical analysis, Journal of Membrane Science 48 (1990) 230–262.
[7] C.R. Bouchard, P.J. Carreau, T. Matsuuara, S. Sourirajan, Modeling of ultrafiltration: predictions of concentration polarization effects, Journal of Membrane Science 97 (1994) 215–227.
[8] S. Bhattacharjee, A. Sharma, P.K. Bhattacharya, Surface interactions in osmotic pressure controlled flux decline during ultrafiltration, Langmuir 10 (1994) 4710–4723.
[9] S. Ganguly, P.K. Bhattacharya, Development of concentration profile and prediction of flux for ultrafiltration in a radial cross flow cell, Journal of Membrane Science 97 (1994) 287–302.
[10] S. Bhattacharya, S.-T. Hwang, Concentration polarization, separation factor, and Peclet number in membrane processes, Journal of Membrane Science 132 (1997) 73–90.

[11] S. De, S. Bhattacharya, A. Sharma, P.K. Bhattacharya, Generalize integral and similarity solutions of the concentration profiles for osmotic pressure controlled ultrafiltration, Journal of Membrane Science 130 (1997) 99–121.
[12] H. Lonsdale, U. Merten, R. Riley, Transport properties of cellulose acetate osmotic membranes, Journal of Applied Polymer Science 9 (1965) 1341–1358.
[13] J.M. Miranda, J.B.L.M. Campos, Concentration polarization in a membrane placed under an impinging jet confined by a conical wall—a numerical approach, Journal of Membrane Science 182 (2001) 257–270.
[14] J.M. Miranda, J.B.L.M. Campos, Mass transfer in the vicinity of a separation membrane—the applicability of the stagnant film theory, Journal of Membrane Science 202 (1–2) (2002) 137–150.
[15] J.M. Miranda, J.B.L.M. Campos, An improved numerical scheme to study mass transfer over a separation membrane, Journal of Membrane Science 188 (2001) 49–59.